

# Tandem droplet locomotion in a uniform electric field

Chiara Sorgentone<sup>1</sup> and Petia M. Vlahovska<sup>2</sup>

<sup>1</sup> *Department of Basic and Applied Sciences for Engineering,  
Sapienza Università di Roma, 00161 Rome, Italy*

<sup>2</sup> *Engineering Sciences and Applied Mathematics, Northwestern University,  
Evanston, IL 60208, USA. Email: petia.vlahovska@northwestern.edu*

(Dated: July 6, 2022)

An isolated charge-neutral droplet in a uniform electric field experiences no net force. However, a droplet pair can move in response to field-induced dipolar and hydrodynamic interactions. If the droplets are identical, the center of mass of the pair remains fixed. Here, we show that if the droplets have different properties, the pair experiences a net motion due to nonreciprocal interactions. We analyze the three-dimensional droplet trajectories using asymptotic theory, assuming spherical droplets and large separations, and numerical simulations based on a boundary integral method. The dynamics can be quite intricate depending on the initial orientation of the droplets line-of-centers relative to the applied field direction. Drops tend to migrate towards a configuration with line-of-centers either parallel or perpendicular to the applied field direction, while either coming into contact or indefinitely separating. We elucidate the conditions under which these different interaction scenarios take place. Intriguingly, we find that in some cases droplets can form a stable pair (tandem) that translates either parallel or perpendicular to the applied field direction.

## I. INTRODUCTION

Electric fields are widely used to steer particles and droplets for applications in directed assembly [1, 2], microfluidics [3, 4], ink-jet printing [5], modulation of emulsion microstructure and rheology [6, 7], and electrosprays [8]. An important issue in practical applications is the droplet interactions due to electric polarization and electrohydrodynamic flows. In the canonical case of an applied uniform electric field, the induced dipoles promote particle chaining along the applied field direction [9, 10]. In addition to the electrostatic interactions, particles may interact electrohydrodynamically due to induced-charge electrophoretic flows in the case of ideally polarizable particles [11] or electric-shear-driven flows about droplets [12]. These flows can be either cooperative or antagonistic to the dipolar interactions [13–16] and prevent chaining [17]. Recently, the three-dimensional interactions of a pair of identical droplets were investigated by means of numerical simulations using the boundary integral method, asymptotic theory for large separations and spherical droplets [16, 18, 19] and experiments [20]. The systematic exploration of the effects of fluid properties and the droplet initial configuration revealed intricate relative motions that eventually lead to either droplet coalescence or indefinite repulsion; only if the droplets line-of-centers were initially perpendicular to the applied field direction and the electrohydrodynamic flow along the droplet surface were equator-to-pole, the drops motion is eventually arrested and the drops remain at an equilibrium separation.

Asymmetry in terms of droplet size or properties is expected to increase the complexity of the droplet interactions, however the problem has been studied only to a limited extent for small droplet deformations and exploring only effects of size difference [20] or only configurations where droplets are aligned with the field [21]. Here, we analyze the three-dimensional interactions of dissimilar drops using both theory and simulations. We find novel dynamics such as droplets “dancing”, where droplets execute complex trajectories before coming into contact or separating, or “swimming”, where droplets form a stable pair that translates in a direction either parallel or perpendicular to the applied field.

## II. PROBLEM FORMULATION

Let us consider two neutrally-buoyant and charge-free drops with radii  $a_i$  and different viscosities  $\eta_{d,i}$ , conductivities  $\sigma_{d,i}$ , and permittivities  $\varepsilon_{d,i}$ , suspended in a fluid with viscosity  $\eta_s$ , conductivity  $\sigma_s$ , and permittivity  $\varepsilon_s$ . The mismatch of drop and suspending fluid properties is characterized by the conductivity, permittivity, and viscosity ratios

$$R_i = \frac{\sigma_{d,i}}{\sigma_s}, \quad S_i = \frac{\varepsilon_{d,i}}{\varepsilon_s}, \quad \lambda_i = \frac{\eta_{d,i}}{\eta_s}, \quad i = 1, 2 \quad (1)$$

The difference in drop size introduces one more parameter,  $\nu = a_2/a_1$ . The distance between the drops’ centroids is  $d$  and the angle between the drops’ line-of-centers with the applied field direction is  $\Theta$ . The unit separation vector between the drops is defined by the difference between the position vectors of the drops’ centers of mass  $\hat{\mathbf{d}} = (\mathbf{x}_2^c - \mathbf{x}_1^c)/d$ . The unit vector normal to the drops line-of-centers and orthogonal to  $\hat{\mathbf{d}}$  is  $\hat{\mathbf{t}}$ .

We adopt the leaky dielectric model, which is widely used to describe the electrohydrodynamics of weakly conducting, viscous fluids [12, 22, 23]. Fluid motion and electric field are described by Stokes and Laplace equations, respectively:

$$\eta \nabla^2 \mathbf{u} - \nabla p = 0, \quad \nabla \cdot \mathbf{E} = 0, \quad (2)$$

where  $\mathbf{u}$  and  $p$  are the fluid velocity and pressure, and  $\mathbf{E}$  is the electric field. Far away from the drops,  $\mathbf{E}^s \rightarrow \mathbf{E}^\infty = E_0 \hat{\mathbf{z}}$  and  $\mathbf{u} \rightarrow 0$ .

At the drop interfaces, normal electric current is continuous, as originally proposed by [24],  $E_n^s = R E_n^d$ , where  $E_n = \mathbf{E} \cdot \mathbf{n}$ , and  $\mathbf{n}$  is the outward pointing normal vector to the drop interface. The surface charge density adjusts to satisfy the current balance, leading to a discontinuity of the displacement field  $\varepsilon^s (E_n^s - S E_n^d) = q$ .

The electric field acting on the induced surface charge  $q$  gives rise to electric shear stress at the interface. The tangential stress balance yields

$$(\mathbf{I} - \mathbf{nn}) \cdot (\mathbf{T}^s - \mathbf{T}^d) \cdot \mathbf{n} + q \mathbf{E}_t = 0, \quad \mathbf{x} \in \mathcal{D}, \quad (3)$$

where  $T_{ij} = -p\delta_{ij} + \eta(\partial_j u_i + \partial_i u_j)$  is the hydrodynamic stress and  $\delta_{ij}$  is the Kronecker delta function. The electric tractions are calculated from the Maxwell stress tensor  $T_{ij}^{\text{el}} = \varepsilon (E_i E_j - E_k E_k \delta_{ij}/2)$ .  $\mathbf{E}_t = \mathbf{E} - E_n \mathbf{n}$  is the tangential component of the electric field, which is continuous across the interface, and  $\mathbf{I}$  is the idemfactor. The normal stress balance is

$$\mathbf{n} \cdot (\mathbf{T}^s - \mathbf{T}^d) \cdot \mathbf{n} + \frac{1}{2} \left( (E_n^s)^2 - S (E_n^d)^2 - (1 - S) E_t^2 \right) = \gamma \nabla_s \cdot \mathbf{n}, \quad \mathbf{x} \in \mathcal{D}, \quad (4)$$

where  $\gamma$  is the interfacial tension.

Henceforth, all variables are nondimensionalized using the radius of the undeformed drops  $a$ , the undisturbed field strength  $E_0$ , a characteristic applied stress  $\tau_c = \varepsilon_s E_0^2$ , and the properties of the suspending fluid. Accordingly, the time scale is  $t_c = \eta_s / \tau_c$  and the velocity scale is  $u_c = a_1 \tau_c / \eta_s$ . The ratio of the magnitude of the electric stresses and surface tension defines the electric capillary number  $Ca_i = \frac{\varepsilon_s E_0^2 a_i}{\gamma}$ .

### III. METHODOLOGY

Our numerical method and the asymptotic theory for identical drops were presented and validated in [16]. Here we summarize the extension of the small-deformation theory and the numerical method to dissimilar drops.

#### A. Integral representation for the velocity

We utilize a Boundary Integral Method (BIM) to solve for the flow and electric fields. Here we derive a boundary integral formulation taking into account the fact that the two drops may have different permittivities and conductivities:

$$\mathbf{E}^\infty(\mathbf{x}) + \sum_{j=1}^2 \int_{\mathcal{D}_j} \frac{\hat{\mathbf{x}}}{4\pi r^3} (\mathbf{E}^s(\mathbf{y}) - \mathbf{E}^i(\mathbf{y})) \cdot \mathbf{n}(\mathbf{y}) dS(\mathbf{y}) = \begin{cases} \mathbf{E}^i(\mathbf{x}) & \text{if } \mathbf{x} \text{ inside } \mathcal{D}_i, \\ \frac{1}{2} (\mathbf{E}^i(\mathbf{x}) + \mathbf{E}^s(\mathbf{x})) & \text{if } \mathbf{x} \in \mathcal{D}_i, \\ \mathbf{E}^s(\mathbf{x}) & \text{if } \mathbf{x} \in S. \end{cases} \quad (5)$$

where  $\hat{\mathbf{x}} = \mathbf{x} - \mathbf{y}$  and  $r = |\hat{\mathbf{x}}|$ . The normal and tangential components of the electric field are calculated from the above equation

$$\frac{(R_i + 1)}{2R_i} E_n(\mathbf{x}) = \mathbf{E}^\infty(\mathbf{x}) \cdot \mathbf{n}(\mathbf{x}) + \sum_{j=1}^2 \frac{R_j - 1}{R_j} \mathbf{n}(\mathbf{x}) \cdot \int_{\mathcal{D}_j} \frac{\hat{\mathbf{x}}}{4\pi r^3} E_n(\mathbf{y}) dS(\mathbf{y}), \quad (6)$$

$$\mathbf{E}_t(\mathbf{x}) = \frac{\mathbf{E}^s(\mathbf{x}) + \mathbf{E}^i(\mathbf{x})}{2} - \frac{1 + R_i}{2R_i} E_n(\mathbf{x}) \mathbf{n}(\mathbf{x}) \quad (7)$$

for  $\mathbf{x} \in \mathcal{D}_i$ . In order to obtain the mean field appearing in eq. (7) we make use of eq. (5) combined with the continuity of normal current across the interface

$$\frac{1}{2} (\mathbf{E}^i(\mathbf{x}) + \mathbf{E}^s(\mathbf{x})) = \mathbf{E}^\infty(\mathbf{x}) + \sum_{j=1}^2 \int_{\mathcal{D}_j} \frac{\hat{\mathbf{x}}}{4\pi r^3} \left( \frac{R_j - 1}{R_j} \right) E_n(\mathbf{y}) dS(\mathbf{y}). \quad (8)$$

For the flow field, we have developed the method for fluids of arbitrary viscosity, but for the sake of brevity here we list the equations in the case of equiviscous drops and suspending fluids. The velocity is given by

$$2\mathbf{u}(\mathbf{x}) = - \sum_{j=1}^2 \left( \frac{1}{4\pi} \int_{\mathcal{D}_j} \left( \frac{\mathbf{f}(\mathbf{y})}{Ca} - \mathbf{f}^E(\mathbf{y}) \right) \cdot \left( \frac{\mathbf{I}}{r} + \frac{\hat{\mathbf{x}}\hat{\mathbf{x}}}{r^3} \right) dS(\mathbf{y}) \right), \quad (9)$$

where  $\mathbf{f}$  and  $\mathbf{f}^E$  are the interfacial stresses due to surface tension and electric field

$$\mathbf{f} = \mathbf{n} \nabla_s \cdot \mathbf{n}, \quad \mathbf{f}^E = (\mathbf{E}^s \cdot \mathbf{n}) \mathbf{E}^s - \frac{1}{2} (\mathbf{E}^s \cdot \mathbf{E}^s) \mathbf{n} - S_i \left( (\mathbf{E}^i \cdot \mathbf{n}) \mathbf{E}^i - \frac{1}{2} (\mathbf{E}^i \cdot \mathbf{E}^i) \mathbf{n} \right). \quad (10)$$

Drop velocity and centroid are computed from the volume averages

$$\mathbf{U}_j = \frac{1}{V} \int_{V_j} \mathbf{u} dV = \frac{1}{V} \int_{\mathcal{D}_j} \mathbf{n} \cdot (\mathbf{u} \mathbf{x}) dS, \quad \mathbf{x}_j^c = \frac{1}{V} \int_{V_j} \mathbf{x} dV = \frac{1}{2V} \int_{\mathcal{D}_j} \mathbf{n} (\mathbf{x} \cdot \mathbf{x}) dS. \quad (11)$$

To solve the system of equations Eq. (6), Eq. (9) we use a Galerkin formulation based on a spherical harmonics representation presented in [18]. All variables (position vector, velocities, electric field) are expanded in spherical harmonics which provides an accurate representation even for relatively low expansion order. In order to deal with the singular and nearly singular integrals that appear in the formulation we evoke specialized quadrature methods able to control the quadrature errors [25], and a reparametrization procedure able to ensure a high-quality representation of the drops also under deformation is used to ensure the spectral accuracy of the method [26].

## B. Asymptotic theory for at large separations

An isolated, charge-neutral drop in a uniform electric field does not move. The proximity of a boundary [27] or another drop breaks the symmetry and can cause droplet migration. However if the drops are identical there is no net motion, i.e., their center of mass remains stationary. Here, we apply the asymptotic theory developed in [16, 20] to dissimilar drops and show that the asymmetry gives rise to cooperative droplet propulsion.

We first evaluate the electrostatic interaction of two widely separated spherical drops. In this case, the drops can be approximated by point-dipoles. The disturbance field  $\mathbf{E}_1$  of the drop dipole  $\mathbf{P}_1$  induces a dielectrophoretic (DEP) force on the dipole  $\mathbf{P}_2$  located at  $\mathbf{x}_2^c = d\hat{\mathbf{d}}$ , given by  $\mathbf{F}_2(d) = (\mathbf{P}_2 \cdot \nabla \mathbf{E}_1)|_{r=d}$ . Likewise, dipole  $\mathbf{P}_2$  induces a force on dipole 1 that is of equal magnitude and opposite sign  $\mathbf{F}_1 = -\mathbf{F}_2$ . The drop velocity under the action of this force can be estimated from Stokes law,  $\mathbf{U}_i = \mathbf{F}_i/\zeta_i$  where  $\zeta$  is the friction coefficient  $\zeta_i = 6\pi(3\lambda_i + 2)/(3(\lambda_i + 1))$ . Thus,

$$\mathbf{U}_i^{\text{dep}} = 2\frac{\beta_D}{d^4} \left( \frac{3(1 + \lambda_i)}{2 + 3\lambda_i} \right) \left[ (1 - 3\cos^2 \Theta) \hat{\mathbf{d}} - \sin(2\Theta) \hat{\mathbf{t}} \right], \quad \beta_D = \left( \frac{R_1 - 1}{R_1 + 2} \right) \left( \frac{R_2 - 1}{R_2 + 2} \right) \quad (12)$$

If  $(R_1 - 1)(R_2 - 1) > 0$ , as in the case of identical droplets, droplets attract if  $\Theta < \Theta_c = \arccos\left(\frac{1}{\sqrt{3}}\right) \approx 54.7^\circ$ , e.g., when the drops are lined up with the field, and repel if the line of centers of the two drops is perpendicular to the applied field. The droplets line-of-centers rotates to align with the applied field. However, this situation reverses if  $(R_1 - 1)(R_2 - 1) < 0$ : the droplets repel if their line-of-centers is parallel the applied field direction, and attract if their line-of-centers is perpendicular to the field. The DEP interaction in this case rotates the droplet line-of-centers away from the applied field direction.

The electrohydrodynamic (EHD) flow about droplet 1 moves droplet 2 and vice versa the flow about droplet 2 moves droplet 1. The velocities of the droplets are

$$\mathbf{U}_2^{\text{ehd}} = \beta_{T,1} \mathbf{U}^{\text{ehd}}(d, \lambda_2), \quad \mathbf{U}_1^{\text{ehd}} = -\beta_{T,2} \mathbf{U}^{\text{ehd}}(d, \lambda_1) \quad (13)$$

where

$$\mathbf{U}^{\text{ehd}}(d, \lambda) = \left( \frac{1}{d^2} - \frac{2}{d^4} \left( \frac{1 + 3\lambda}{2 + 3\lambda} \right) \right) (-1 + 3\cos^2 \Theta) \hat{\mathbf{d}} - \frac{2}{d^4} \left( \frac{1 + 3\lambda}{2 + 3\lambda} \right) \sin(2\Theta) \hat{\mathbf{t}} + O(d^{-5}). \quad (14)$$

and the stresslet magnitude is

$$\beta_{T,i} = \frac{9}{10} \frac{R_i - S_i}{(1 + \lambda_i)(R_i + 2)^2}, \quad i = 1, 2 \quad (15)$$

For equiviscous droplets, the relative velocity  $\mathbf{U}_2 - \mathbf{U}_1$  shows that the EHD interaction changes sign (attractive to repulsive or vice versa depending on  $\beta_{T,2} + \beta_{T,1}$ ) at the same critical angle  $\Theta_c$  as the DEP case. However, the EHD interaction also changes sign at separation  $d_c^2 = 2(1 + 3\lambda)/(2 + 3\lambda)$ .  $d_c$  ranges from 1 for bubbles ( $\lambda = 0$ ) to  $\sqrt{2}$  for very viscous drops ( $\lambda \rightarrow \infty$ ), both corresponding to center-to-center distance smaller than the minimal separation of 2 for spherical drops. Accordingly, in reality the sign of the EHD interactions does not vary with drop-drop separation. For droplets aligned with the field, both  $\beta_T$  negative results in EHD attraction, since the surface flow about each drop is from pole to equator and the fluid is being drawn away from the space between the droplets. Both  $\beta_T$  positive results in repulsion because the surface flow about the droplets is equator to pole and the fluid is being drawn into the space between the droplets, effectively pushing them away. Dissimilar droplets can either attract or repel depending the relative strength of their stresslets. These scenarios reverse for droplet with line-of-centers perpendicular to the applied field direction.

## IV. RESULTS

In this section, we explore the pair-wise droplet dynamics using the analytical theory and numerical simulations.

### A. Droplet cooperative propulsion

Dissimilarity creates nonreciprocal interactions which give rise to a net motion of the pair. The “swimming” velocity, defined as the velocity of the pair center-of-mass, at leading order is

$$\mathbf{U}_s = \frac{1}{2} (\mathbf{U}_2 + \mathbf{U}_1) = f(d) (-1 + 3\cos^2 \Theta) \hat{\mathbf{d}} + g(d) \sin(2\Theta) \hat{\mathbf{t}}. \quad (16)$$

The most natural source of dissimilarity is a difference in droplet size. In this case, for droplets with same material properties

$$\begin{aligned} f(d) &= -\frac{\beta_T}{d^2}(\nu^3 - 1) + \frac{1}{d^4(2 + 3\lambda)} (\beta_T(1 + 3\lambda)(\nu^5 - 1) + 3\beta_D(1 + \lambda)(\nu^3 - 1)) , \\ g(d) &= \frac{1}{d^4(2 + 3\lambda)} (\beta_T(1 + 3\lambda)(\nu^5 - 1) + 3\beta_D(1 + \lambda)(\nu^3 - 1)) \end{aligned} \quad (17)$$

where  $\nu$  is the ratio of droplet radii.

Difference in droplet viscosity also breaks the symmetry and drives self-propulsion. In this case, if all other properties and drop radii are the same, the swimming speed is controlled by the viscosity mismatch of the droplets

$$f(d) = g(d) = \frac{3(\lambda_1 - \lambda_2)}{d^4(2 + 3\lambda_1)(2 + 3\lambda_2)} (-\beta_T + \beta_D) . \quad (18)$$

The swimming direction and speed are controlled by the relative importance of the induced dipole and the EHD stresslet. The EHD flow weakens with increasing conductivity, and for  $R \rightarrow \infty$ ,  $-\beta_T + \beta_D \rightarrow 1$ . The DEP interaction vanishes at  $R = 1$ , and in this case the swimming is driven by the interaction of the droplets stresslet flows.

Here, we focus on droplets with same size and viscosity but different conductivities and permittivities. In this case, the DEP interactions cancel out and the swimming speed is set by the droplet stresslets

$$\mathbf{U}_s = \frac{1}{2} (\mathbf{U}_2 + \mathbf{U}_1) = \frac{1}{2} (\beta_{T,1} - \beta_{T,2}) \mathbf{U}^{\text{ehd}} . \quad (19)$$

Hence, the nonreciprocal electrohydrodynamic interaction is the source of the droplet tandem locomotion; the swimming speed vanishes if the droplet stresslets are the same. The direction of motion is determined by the stresslets difference. For example, droplets with  $R_1 = 0.1$ ,  $R_2 = 100$  and same permittivity ratio ( $S_1 = S_2 = 1$ ) that are initially aligned with the field translate antiparallel to the field ; swapping the droplets reverses the swimming direction. In this case, droplets settle into a stable separation. In general, however, the drop pair dynamics is complex because the center-of-mass motion is superimposed on changes in separation and rotation of the line-of-centers relative to applied field direction.

## B. Droplet trajectories

Here we examine the conditions to form a stable locomoting tandem. According to the theory, the droplet separation and line-of-center orientation evolve as

$$\dot{d} = \mathbf{U} \cdot \hat{\mathbf{d}} = \left[ (\beta_{T,1} + \beta_{T,2}) \frac{1}{d^2} - \frac{2}{d^4} \Phi(\lambda, d) \right] (-1 + 3 \cos^2 \Theta) \quad (20)$$

$$\dot{\Theta} = \frac{1}{d} \mathbf{U} \cdot \hat{\mathbf{t}} = -\frac{2}{d^5} \Phi(\lambda, d) \sin(2\Theta) \quad (21)$$

where  $\mathbf{U} = \mathbf{U}_2 - \mathbf{U}_1$  is the relative velocity and

$$\Phi(\lambda, d) = \left( \frac{1 + 3\lambda}{2 + 3\lambda} \right) \left[ (\beta_{T,1} + \beta_{T,2}) + 2\beta_D \left( \frac{3(1 + \lambda)}{1 + 3\lambda} \right) \right] . \quad (22)$$

Examination of this dynamical system shows that there are two equilibrium points:  $\Theta_* = 0$  and  $d_* = d_{\text{eq}}$ , and  $\Theta_* = \pi/2$  and  $d_* = d_{\text{eq}}$ , where (for viscosity ratio 1)

$$d_{\text{eq}}^2 = \frac{8}{5} + \frac{32(R_1 - 1)(R_1 + 2)(R_2 - 1)(R_2 + 2)}{3(R_1^2(R_2 - S_2) + R_1(R_2(R_2 + 8) - 4S_2 + 4) + R_2(4 - (R_2 + 4)S_1) - 4(S_1 + S_2))} \quad (23)$$

The equilibrium points are saddles, as seen from the phase plane plotted in Fig. 1. If the droplet line-of-centers is initially aligned with the applied field direction, the droplets attain a steady separation for values of the droplet conductivities corresponding to Fig. 1 (c) and the left branch of Fig. 1(b). If the droplet line-of-centers is initially perpendicular to the applied field direction the steady separation is given by the right branch of Fig. 1(b). In these

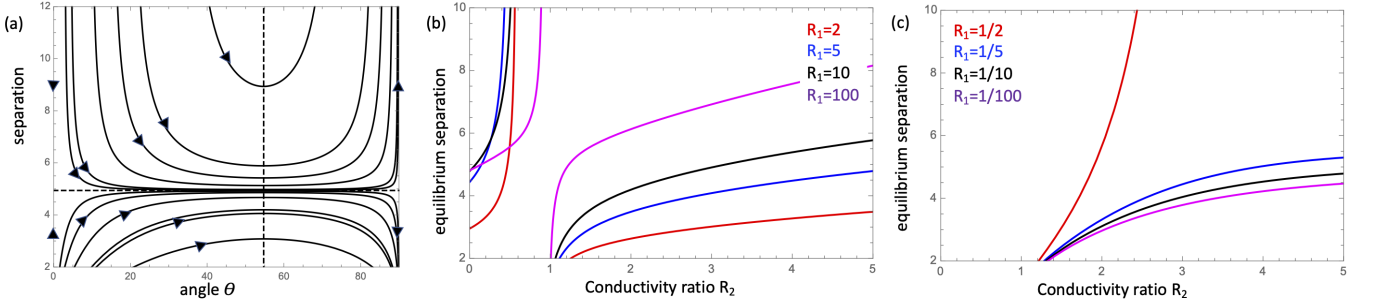


FIG. 1. (a) Phase plane of droplet trajectories for  $R_1 = 0.1$ ,  $R_2 = 100$  and  $S_1 = S_2 = 1$ , corresponding to  $\Phi < 0$ . (b) and (c) Equilibrium separation  $d_{eq}$  for drops with different conductivity but same permittivity  $S_1 = S_2 = 1$ .

scenarios, the DEP is repulsive and stronger than the EHD at short separations and the EHD is attractive at large separations. Accordingly, the drops attract or repel until they reach the equilibrium separation  $d_{eq}$ .

Any misalignment of the drops line-of-centers drives the droplets away from the equilibrium configurations towards contact or infinite separation. The trajectories  $d(\Theta)$  are given by

$$d^2(\Theta, d_0, \Theta_0) = \frac{f(\Theta, d_0, \Theta_0)}{1 + 2bf(\Theta, d_0, \Theta_0)}, \quad (24)$$

where

$$f(\Theta, d_0, \Theta_0) = \frac{d_0^2}{1 - 2bd_0^2} \left( \frac{\cos \Theta \sin^2 \Theta}{\cos \Theta_0 \sin^2 \Theta_0} \right), \quad b = \frac{5(\beta_{T,1} + \beta_{T,2})}{16(\beta_{T,1} + \beta_{T,2} + 3\beta_D)}.$$

In the case  $\Phi < 0$ , if the initial separation  $d_0 > d_{eq}$ , the droplets either initially attract but then separate indefinitely if  $\Theta_0 < \Theta_c$  or monotonically separate if  $\Theta_0 > \Theta_c$ . This scenario is reversed if  $d_0 < d_{eq}$ , where droplets ultimately come into contact. However, if the drops are misaligned but separated exactly by  $d_{eq}$ , i.e.,  $d = d_0$ , their separation remains constant while their line-of-centers rotates continuously towards the equilibrium points, either  $\Theta_* = 0$ , if  $\Phi > 0$ , or  $\Theta_* = \pi/2$ , in the opposite case, see Eq. (21).

Figures 2 and 3 illustrate the droplet dynamics for the cases  $\Phi < 0$  and  $\Phi > 0$ . If  $\Phi < 0$  and  $\Theta_0 = 0$  drops form a steady-pair configuration. For  $\Theta_0 \neq 0$ , the misaligned droplets migrate towards a configuration where the line-of-centers is nearly perpendicular to the field. In the initial configuration, the induced dipoles are directed in opposite direction, resulting in DEP repulsion. The stresslets also have opposite sign, however the EHD flow for the  $R = 0.1$  droplet is stronger and its pole-to-equator surface flow results in attraction between the drops. If the initial distance between the drops is greater than the equilibrium separation,  $d_0 > d_{eq}$ , the interaction is initially dominated by the EHD and droplets attract. However, as they get closer the DEP repulsion intensifies and causes them to repel and indefinitely separate, while drop 1 is “chasing” drop 2, with decreasing swimming speed. If  $\Theta_0 < \Theta_c$ , the droplets initially attract before starting to repel, see Fig. 2(top); if  $\Theta_0 > \Theta_c$  the repulsion is monotonic. In the opposite case,  $d_0 < d_{eq}$ , the interactions are reversed: the droplets initially repel and then attract (if  $\Theta_0 < \Theta_c$ ), or monotonically attract (if  $\Theta_0 > \Theta_c$ ), and eventually come in contact. The droplets relative velocity increases rapidly as they approach each other, see Fig. 2(bottom). The swimming speed varies along the trajectories and it is minimal when the radial velocity is close to zero. Comparison of the numerical and theoretical results shows that the asymptotic theory qualitatively captures the drop dynamics. The agreement between simulations and theory is better for droplets that are initially farther apart. Thus, given the high computational costs of the simulations, the theory can be used to estimate droplet interactions. Droplet deformation increases the  $d_{eq}$  above which drops evolve towards separating state. In the considered example, we found by numerical simulations that  $d_0 = 6$  also leads to contact since the deformation causes the drops to get too close and unable to escape the DEP attraction which ultimately leads to contact.

In the case of droplets pairing in transverse direction,  $\Phi > 0$ , the droplets exhibit the opposite orientational behavior and move to align with the field. If the initial separation is smaller than the equilibrium one, drops come in contact, and otherwise separate indefinitely, while both drops move in opposite direction (“run away” from each other), see Fig. 3. In the latter case, the interaction is extremely weak. The trajectory time is 500000, which is prohibitively expensive to simulate numerically.

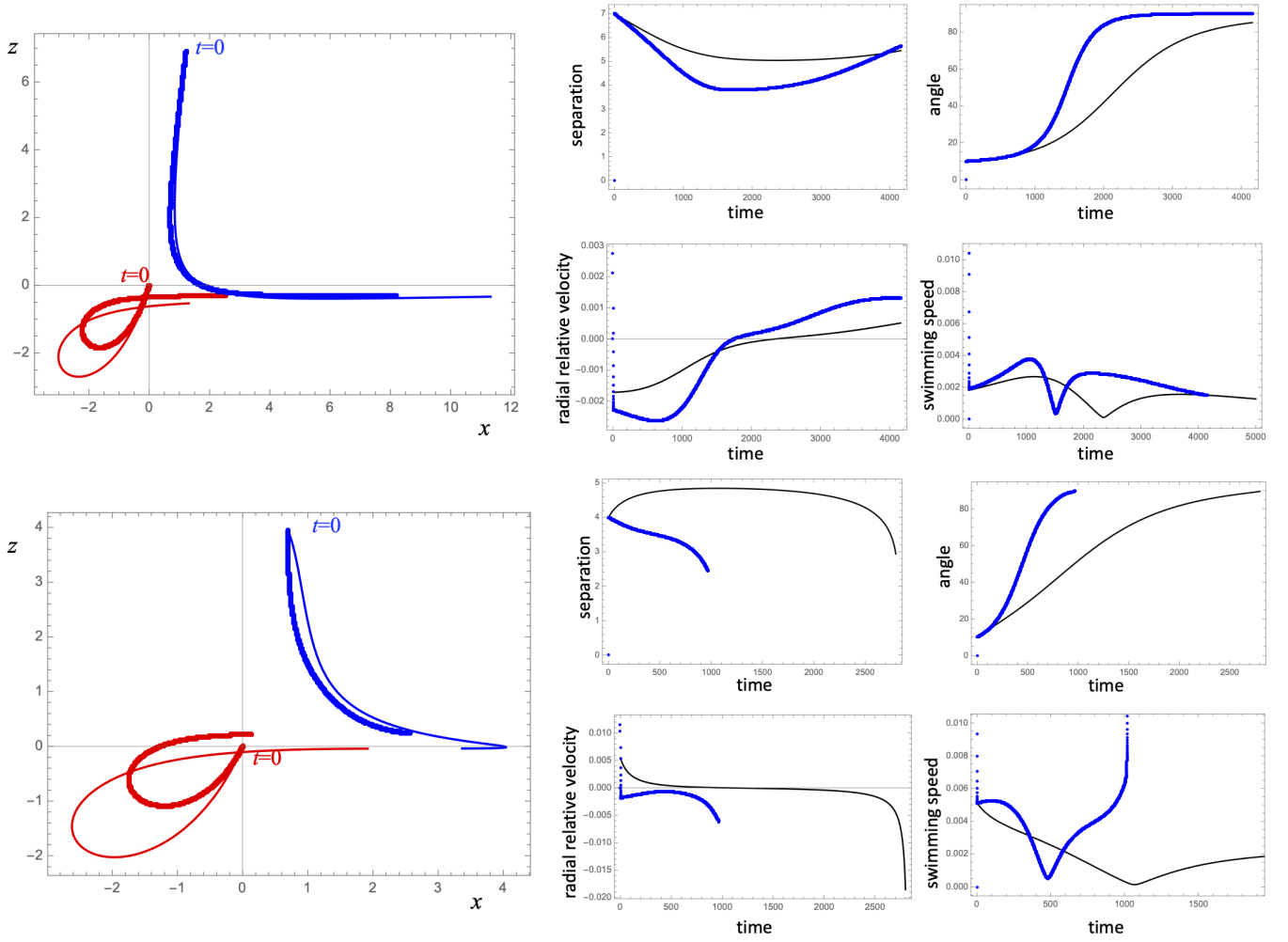


FIG. 2. Droplet-pair dynamics for  $R_1 = 0.1$ ,  $R_2 = 100$ ,  $S_1 = S_2 = 1$ ,  $\lambda_1 = \lambda_2 = 1$  and initial angle  $\Theta_0 = 10^\circ$ . For this system  $d_{eq} = 4.94$ . Lines are computed from the asymptotic theory. Symbols correspond to the numerical simulations. Initial separation is  $d_0 = 7$  (top) and  $d_0 = 4$  (bottom).

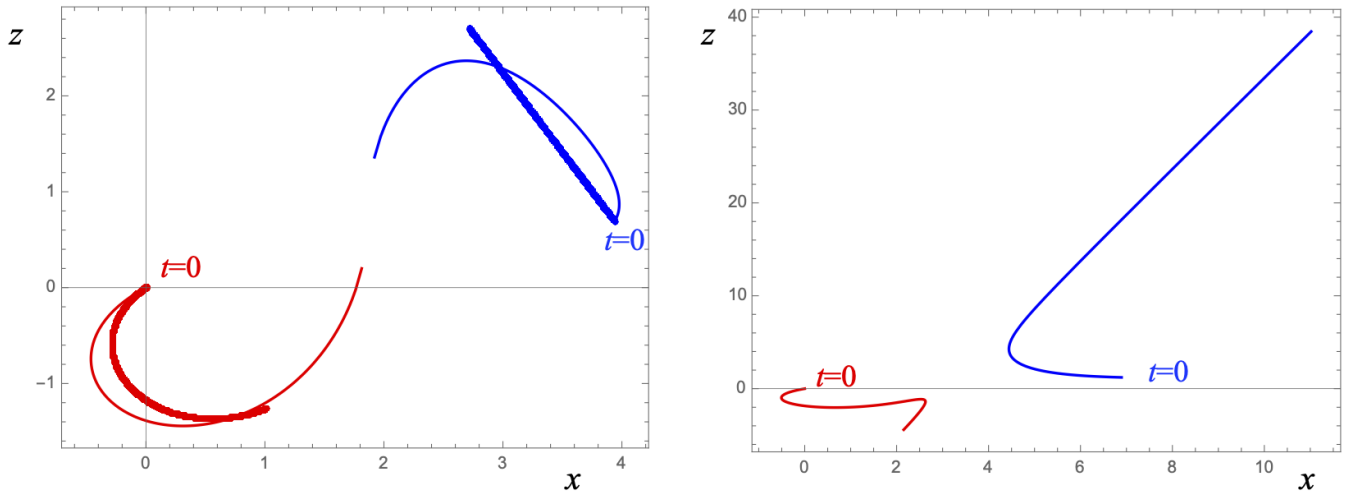


FIG. 3. Droplet-pair dynamics for  $R_1 = 2$ ,  $R_2 = 100$ ,  $S_1 = S_2 = 1$ ,  $\lambda_1 = \lambda_2 = 1$ , and initial angle  $\Theta_0 = 80^\circ > \Theta_c$ . Initial separation (left)  $d_0 = 4$ , leading to contact, and (right)  $d_0 = 7$ , leading to indefinite separation. Symbols correspond to the numerical simulations. Trajectories computed from the asymptotic theory are over period of time 2228 (left) and 500000 (right).

## V. CONCLUSIONS

We analyze the interactions of dissimilar droplets in a uniform electric field by means of an asymptotic theory, assuming spherical droplets ( $Ca \ll 1$ ) and large separations, and numerical simulations, using a three-dimensional Boundary Integral Method. The simulations for  $Ca = 0.1$  qualitatively agree with the theory, and thus the theory can be used for a fast estimate of the drop trajectories. Our study focuses on the effect of the mismatch in the electric properties, considering drops with different conductivity and permittivity but same size and viscosity. In this case, the nonreciprocal electrohydrodynamic interactions give rise to a net motion of the drop pair. The center-of-mass motion is accompanied by changes in drop separation and angle between their line-of-centers to the applied field direction, which gives rise to intricate trajectories. Depending on the droplet stresslets and dipoles in the function  $\Phi$ , defined by Eq. (22), drops tend to orient their line-of-centers either parallel, if  $\Phi > 0$ , or perpendicular to the applied field direction, if  $\Phi < 0$ . Initial separation determines if drops will coalesce or indefinitely separate. For drops with  $\Phi < 0$ , if  $d_0 > d_{eq}$  and  $\Theta_0 < \Theta_c$ , drops initially attract and then separate indefinitely, while chasing each other. If  $d_0 < d_{eq}$  and  $\Theta_0 < \Theta_c$ , droplets repel and then attract until contact; the interaction is purely attractive and separation decreases monotonically if  $\Theta_0 > \Theta_c$ . In the particular case of drops aligned with the field and  $\Phi < 0$ , the drops reach steady separation and “swim” along the applied field direction, if  $R_1 < R_2$ ; direction of motion is reversed if  $R_1 > R_2$ . If  $\Phi > 0$  and the drops line-of-centers is perpendicular to the applied field direction the droplet form a tandem swimming transversely to the field. If instead the drops line-of-centers is initially misaligned with the applied field direction, with  $d_0 > d_{eq}$  and  $\Theta_0 > \Theta_c$ , drops initially attract, then repel indefinitely while moving in opposite directions of each other. If  $d_0 < d_{eq}$  and  $\Theta_0 > \Theta_c$ , droplets first repel and then attract until contact. In both cases, the separation changes monotonically if  $\Theta_0 < \Theta_c$ .

Our work represents the first study of the three-dimensional dynamics of electrically dissimilar drops and opens new directions of exploration of how to manipulate droplets and direct assembly of particles with electric fields.

## VI. ACKNOWLEDGMENTS

PV has been supported in part by NSF award CBET-2126498.

## VII. DECLARATION OF INTERESTS

The authors report no conflict of interest.

- 
- [1] A. van Blaaderen, M. Dijkstra, R. van Roij, A. Imhof, M. Kamp, B. W. Kwaadgras, T. Vissers, and B. Liu. Manipulating the self assembly of colloids in electric fields. *Eur. Phys. J -Special Topics*, 222(11):2895–2909, NOV 2013. ISSN 1951-6355. doi:10.1140/epjst/e2013-02065-0.
  - [2] A. A. Harraq, B. D. Choudhury, and B. Bharti. Field-induced assembly and propulsion of colloids. *Langmuir*, 38(10):3001–3016, 2022. doi:10.1021/acs.langmuir.1c02581. URL <https://doi.org/10.1021/acs.langmuir.1c02581>. PMID: 35238204.
  - [3] DR Link, E. Grasland-Mongrain, A Duri, F Sarrazin, ZD Cheng, G Cristobal, M Marquez, and DA Weitz. Electric control of droplets in microfluidic devices. *ANGEWANDTE CHEMIE-INTERNATIONAL EDITION*, 45(16):2556–2560, 2006. ISSN 1433-7851. doi:10.1002/anie.200503540.
  - [4] Johannes Hartmann, Maximilian T. Schuer, and Steffen Hardt. Manipulation and control of droplets on surfaces in a homogeneous electric field. *NATURE COMMUNICATIONS*, 13(1), JAN 12 2022. doi:10.1038/s41467-021-27879-0.
  - [5] O. A. Basaran, H. Gao, and P. P. Bhat. Nonstandard Inkjets. *Annu. Review Fluid Mech.*, 45:85–113, 2013. ISSN 0066-4189. doi:10.1146/annurev-fluid-120710-101148.
  - [6] J. S. Eow and M. Ghadiri. Electrostatic enhancement of coalescence of water droplets in oil: a review of the technology. *Chem. Eng. Sci.*, 85:357–368, 2002.
  - [7] Rongjia Tao, Hong Tang, Kazi Tawhid-Al-Islam, Enpeng Du, and Jeongyoo Kim. Electrorheology leads to healthier and tastier chocolate. *Proceedings of the National Academy of Sciences*, 113(27):7399–7402, 2016. doi:10.1073/pnas.1605416113. URL <https://www.pnas.org/doi/abs/10.1073/pnas.1605416113>.
  - [8] Alfonso M. Ganan-Calvo, Jose M. Lopez-Herrera, Miguel A. Herrada, Antonio Ramos, and Jose M. Montanero. Review on the physics of electrospray: From electrokinetics to the operating conditions of single and coaxial taylor cone-jets, and ac electrospray. *Journal of Aerosol Science*, 125:32–56, 2018. ISSN 0021-8502. doi:<https://doi.org/10.1016/j.jaerosci.2018.05.002>. URL <http://www.sciencedirect.com/science/article/pii/S0021850217304305>.



- [9] C F Zukoski. Material properties and the electrorheological response. *Annual Review of Materials Science*, 23(1):45–78, 1993. doi:10.1146/annurev.ms.23.080193.000401. URL <https://doi.org/10.1146/annurev.ms.23.080193.000401>.
- [10] Ping Sheng and Weijia Wen. Electrorheological Fluids: Mechanisms, Dynamics, and Microfluidics Applications. In Davis, SH and Moin, P, editor, *ANNUAL REVIEW OF FLUID MECHANICS, VOL 44*, volume 44 of *Annual Review of Fluid Mechanics*, pages 143+. 2012. ISBN 978-0-8243-0744-8. doi:10.1146/annurev-fluid-120710-101024.
- [11] T. M. Squires and M. Z. Bazant. Induced-charge electro-osmosis and electrophoresis. *J. Fluid Mech.*, 509:217–252, 2004.
- [12] J. R. Melcher and G. I. Taylor. Electrohydrodynamics - a review of role of interfacial shear stress. *Annu. Rev. Fluid Mech.*, 1:111–146, 1969.
- [13] J. C. Baygents, N. J. Rivette, and H. A. Stone. Electrohydrodynamic deformation and interaction of drop pairs. *J. Fluid. Mech.*, 368:359–375, 1998.
- [14] David Saintillan. Nonlinear interactions in electrophoresis of ideally polarizable particles. *Phys. Fluids*, 20(6), JUN 2008. ISSN 1070-6631. doi:10.1063/1.2931689.
- [15] Jae Sung Park and David Saintillan. Dipolophoresis in large-scale suspensions of ideally polarizable spheres. *JOURNAL OF FLUID MECHANICS*, 662:66–90, NOV 10 2010. ISSN 0022-1120. doi:10.1017/S0022112010003137.
- [16] C. Sorigtone, Jeremy I. Kach, Aditya S. Khair, Lynn M. Walker, and Petia M. Vlahovska. Numerical and asymptotic analysis of the three-dimensional electrohydrodynamic interactions of drop pairs. *J. Fluid Mech.*, 914:A24, 2021.
- [17] J.-W. Ha and S.-M. Yang. Rheological responses of oil-in-oil emulsions in an electric field. *J. Rheol.*, 44:235–256, 2000.
- [18] C. Sorigtone, A.-K. Tornberg, and Petia M. Vlahovska. A 3D boundary integral method for the electrohydrodynamics of surfactant-covered drops. *J. Comp. Phys.*, 389: 111–127, 2019.
- [19] C. Sorigtone and Petia M. Vlahovska. Pairwise interactions of surfactant-covered drops in a uniform electric field. *Phys. Rev. Fluids*, 5:053601, 2021.
- [20] Jeremy I. Kach, Lynn M. Walker, and Aditya S. Khair. Prediction and measurement of leaky dielectric drop interactions. *Phys. Rev. Fluids*, 7:013701, Jan 2022. doi:10.1103/PhysRevFluids.7.013701. URL <https://link.aps.org/doi/10.1103/PhysRevFluids.7.013701>.
- [21] Michael Zabaranin. Small deformation theory for two leaky dielectric drops in a uniform electric field. *Proc. Royal Soc. A*, 476(2233), JAN 8 2020. ISSN 1364-5021. doi:10.1098/rspa.2019.0517.
- [22] D. A. Saville. Electrohydrodynamics: The Taylor-Melcher leaky dielectric model. *Annu. Rev. Fluid Mech.*, 29:27–64, 1997.
- [23] Petia M. Vlahovska. Electrohydrodynamics of drops and vesicles. *Annu. Rev. Fluid Mech.*, 51: 305–330, 2019.
- [24] G. I. Taylor. Studies in electrohydrodynamics. I. Circulation produced in a drop by an electric field. *Proc. Royal Soc. A*, 291:159–166, 1966.
- [25] Ludvig af Klinteberg, Chiara Sorigtone, and Anna-Karin Tornberg. Quadrature error estimates for layer potentials evaluated near curved surfaces in three dimensions. *Computers & Mathematics with Applications*, 111:1–19, 2022. ISSN 0898-1221. doi:<https://doi.org/10.1016/j.camwa.2022.02.001>. URL <https://www.sciencedirect.com/science/article/pii/S0898122122000517>.
- [26] C. Sorigtone and A.-K. Tornberg. A highly accurate boundary integral equation method for surfactant-laden drops in 3D. *J. Comp. Phys.*, 360:167–191, MAY 1 2018. ISSN 0021-9991. doi:10.1016/j.jcp.2018.01.033.
- [27] Ehud Yariv. “force-free” electrophoresis? *Physics of Fluids*, 18(3):031702, 2006. doi:10.1063/1.2185690. URL <https://doi.org/10.1063/1.2185690>.